

# **Characterization of nanoscale property variations in polymer composite systems: Part 1 -- Experimental Results**

M. R. VanLandingham; Center for Composite Materials and Materials Science Program, University of Delaware; current address: National Institute of Standards and Technology, Building Materials Division, Building 226, Room B350, Gaithersburg, MD, 20899; phone: (301) 975-4686; fax: (301) 990-6891.

R. R. Dagastine; Center for Composite Materials and Department of Chemical Engineering, University of Delaware; current address: Department of Chemical Engineering, Carnegie Mellon University, Pittsburgh, PA 15213-3890; phone: (412) 268-3855; fax: (412) 268-7139.

R. F. Eduljee; Center for Composite Materials and Materials Science Program, University of Delaware; 202 Composites Manufacturing Science Laboratory, Newark, DE, 19716-3144; phone: (302) 831-8701; fax: (302) 831-8525.

R. L. McCullough; Center for Composite Materials, Materials Science Program, and Department of Chemical Engineering, University of Delaware; 202 Composites Manufacturing Science Laboratory, Newark, DE, 19716-3144; phone: (302) 831-2765; fax: (302) 831-8525.

J. W. Gillespie, Jr.; Center for Composite Materials and Materials Science Program, University of Delaware; 202 Composites Manufacturing Science Laboratory, Newark, DE, 19716-3144; phone: (302) 831-8702; fax: (302) 831-8525.

## *ABSTRACT*

A technique utilizing the indenting capabilities of the atomic force microscope is used to evaluate local changes in response of polymer composite systems near the fiber-matrix interface. Room-temperature and elevated-temperature indentation response is measured for several model composite systems. Results of indentation studies are compared to finite element model predictions to understand the influence of interphase properties on the measured responses. For sized fiber systems, unexpected property variations are

observed, leading to the discovery of a possible interphase formation mechanism in these systems.

**Key words:** indentation; fiber-matrix interface; interphase regions

**Abbreviated Title:** Property Variations in Polymer Composites: Part 1

## *INTRODUCTION*

The use of polymers in composite materials and adhesives requires sensitive nanoscale property evaluation of polymer systems. In these systems, nanoscale properties that control various aspects of material performance can be different from bulk properties. For example, the behavior of polymer composites is highly dependent on the interfacial strength between the fiber and matrix. However, interfacial strength is controlled by the matrix material adjacent to the fiber, i.e., the fiber-matrix interphase region. In some epoxy matrix systems, fiber-matrix interphase regions form because of preferential adsorption of reacting species to the fiber<sup>1-3</sup>. Models have predicted that this process leads to compositional gradients near the fiber surface<sup>4, 5</sup>, as shown in Figure 1. Recent experimental results using neutron reflectivity have verified these modeling predictions for several epoxy-amine systems reinforced with unsized carbon fibers<sup>1</sup>. From these results, compositional gradients were observed to extend only a few nanometers away from the fiber for each of the systems studied. However, the local microstructure can be altered significantly, causing property differences between the interphase region and the bulk matrix<sup>6</sup>; e.g., a lower interphase glass transition temperature,  $T_g$ .

Experimental evidence of the property differences between the interphase region and the bulk matrix has been obtained using several different methods<sup>7-15</sup>, each of which infer interphase properties indirectly from the test data. The atomic force microscope (AFM) has the ability to measure differences in response directly.

Traditionally, the AFM has been used as a nanoscale profilometer, measuring the topography of surfaces through direct contact between the sample surface and a probe tip mounted on the end of a cantilever microbeam. Development of the AFM's imaging capabilities has focused on the tip-surface interaction forces, leading to the utilization of the AFM as a surface force apparatus. This mode of operation, termed force mode, is generally used to minimize tip-sample forces during imaging. Information regarding the tip-sample forces is given by a force curve, which is a plot of tip deflection as a function of the motion of the piezoelectric actuator in the z direction. Recent developments in software and hardware have been made that allow for nanoscale indentation studies to be performed using the AFM in force mode<sup>6, 16, 17</sup>.

In this paper, the indentation response near fibers in three composite systems is measured using the AFM. These measurements are made at room temperature and at several elevated temperatures using a heating stage, the design of which is described in the following section. In the companion paper, a three-dimensional finite element model of indentation near a fiber is presented. This model is then used to predict interphase effects on indentation response, and the results are compared to experimental measurements.

## *EXPERIMENTAL*

### *Indentation Measurements*

Indentation of several polymer composite systems was performed with the AFM using a technique described in detail elsewhere<sup>6, 16, 17</sup>. In this study, AFM force curves were produced from the interactions between single-fiber composite samples and ultrastiff silicon cantilever probes, for which the estimated spring constants,  $k_c$ , ranged from 200-500 N/m. For each study, indentations were made across a sample surface moving toward the fiber edge with increments in lateral distance ranging from 50 to 400

nm. Several rows of indents were made to study interphases between the fiber and matrix, the fiber and coating, and the matrix and coating, where applicable. Note that the minimum spacing between indentations is limited such that the impressions created due to plastic deformation do not overlap. Increased spatial resolution can be achieved by performing numerous rows of indents across an interphase or by indenting across an interphase at an acute angle. Both of these techniques have been used in the studies of single-fiber specimens. In addition to these rows, at least 10 indents were made on the matrix material several fiber diameters away from the fiber to characterize the bulk matrix response.

For a sample which is infinitely stiff with respect to the probe, no indentation will occur. The measured response is thus characteristic of the AFM probe and the operating conditions and can be used to calibrate the measured indentation responses for the sample of interest<sup>6, 16, 17</sup>. For each composite sample, the fiber cross-section provided an adequate "infinitely stiff" region to calibrate the indentation measurements. At least 10 force curves were obtained for the fiber before and after performing indentation on matrix and interphase regions. Also, each row of indents generally contained indents on the fiber, the responses from which were also used to check the system calibration.

To compare interphase and bulk matrix responses, the displacement recovered during unloading is assumed to be purely elastic. The total indentation displacement,  $\Delta z_i$ , recovered from  $P = P_{\max}$  to  $P = 0$ , where  $P$  is the applied load, is used as a relative measure of sample stiffness. For two separate indentations made on a single sample, the ratio of local elastic modulus values,  $E_1$  and  $E_2$ , is related to the ratio of unloading displacements,  $(\Delta z_i)_1$  and  $(\Delta z_i)_2$ :

$$\frac{(\Delta z_i)_2}{(\Delta z_i)_1} = \frac{r_1 E_1}{r_2 E_2} \quad (1)$$

where  $r_1$  and  $r_2$  are the contact radius values. This equation is valid only under the following three conditions: (1)  $P_{\max}$  is the same for both indents; (2) Poisson's ratio does not change significantly across the sample; and (3) the unloading responses are characterized by power law expressions,  $P = \alpha(z_i)^m$ , for which the resulting power law exponents,  $m$ , are the same<sup>6, 16, 17</sup>. The AFM indentation system is essentially force controlled, as opposed to displacement controlled. Thus,  $P_{\max}$  can be controlled to  $\pm 1\%$  or better accuracy, assuring that condition 1 is met. Note that values of  $P_{\max}$  ranged between 5 and 10  $\mu\text{N}$  depending on the stiffness of the cantilever used in a particular study. The coating and bulk epoxy materials, described in the following subsection, are very similar and thus condition 2 should hold, even where slight compositional variations exist.

To assure that condition 3 was not violated, 10-20 indents were made at large distances from the fiber, i.e. in the bulk epoxy, for each study. Each of these responses was characterized by the maximum load,  $P_{\max}$ , the total unloading displacement,  $\Delta z_i$ , and the power law exponent,  $m$ , of the unloading curve. The distribution of  $m$  values is then determined. For example, for several of the studies, the average value,  $\langle m \rangle$ , was between 1.5 and 1.6 with standard deviations,  $\sigma$ , between 0.04 and 0.07. A response measured near the fiber is compared to the average bulk response only when the corresponding  $m$  value falls within  $\langle m \rangle \pm 2\sigma$ . If so, then the conditions corresponding to Equation 1 are met.

Further, the condition of similar  $m$  values signifies that the geometry controlling the unloading processes for different indentations is similar. This indentation geometry, which is characterized by the contact radius,  $r$ , is a function of the tip geometry and the plastic deformation created during loading<sup>18</sup>. Assuming the tip geometry does not change from indent to indent, the relative changes in indent size can be used to relate contact radius values. Therefore, measurements of indent sizes were made using AFM

images of the indents. Indent size was characterized by the lateral distance from the apex to the base of the triangular impression. In general, indent size did not vary across the sample surfaces so that the ratio,  $r_1/r_2$ , was set to unity in Equation 1. The relative or normalized stiffness,  $E/E_{\text{bulk}}$ , was then calculated by dividing the average  $\Delta z_i$  value for the bulk epoxy by  $\Delta z_i$  for each indent near the fiber (see Equation 1).

### *Materials*

The fiber systems that are studied included unsized and sized AS4 carbon fibers and sized copper fibers. The sized fibers were coated with EPON 1001F epoxy (Shell Corp.) using a 10% by weight solution of EPON 1001F in methylene chloride. The coating procedure consistently yielded 10  $\mu\text{m}$  coatings on the 100  $\mu\text{m}$ -diameter copper wires and 1  $\mu\text{m}$  coatings on the 7  $\mu\text{m}$ -diameter carbon fibers, as confirmed using scanning electron and atomic force microscopy<sup>5, 6</sup>. Single-fiber samples were then processed in the form of single-fiber fragmentation dog bone specimens with the fiber system of interest mounted in a stoichiometric mixture of EPON 828 epoxy (Shell Corp.) and PACM 20 amine curing agent (Air Products, Inc). Note that the coating epoxy, EPON 1001F, is similar to the matrix epoxy, EPON 828, but with a higher molecular weight<sup>5</sup>. Each sample was cured for 2 hours at 80°C and then postcured for 2 hours at 160°C. The single-fiber dog bone samples were then sectioned perpendicular to the fiber axis, mounted in an epoxy potting compound, and polished to a 0.05  $\mu\text{m}$  finish. Indentation responses were then measured for each sample as has been described.

### *Heating stage*

A heating stage for the AFM was designed and constructed to allow for indentation studies to be conducted at elevated temperatures. As shown in Figure 2, this heating stage is composed of a long copper flange mounted on top of a heating element that is mounted on an aluminum plate. The heating element consists of an electrical

resistance coil encased in a high-temperature polyimide film with an adhesive backing, and the copper flange and aluminum plate are insulated using an alumina silica paper insulation. Thus, heat is conducted down the copper flange to the bottom of the sample, and the piezoelectric actuator of the AFM is virtually isolated from any electro-magnetic fields created by the heating element. An optimum sample height range was determined to be 3-7 mm based on the required watt densities and the temperature limitations of the sample<sup>19</sup>. The overall diameter of a potted sample is approximately 3 cm.

The sample is placed near the end of the copper flange, taped down to the copper with high temperature polyimide tape, and surrounded by insulation. To improve thermal contact between the bottom of the sample and the copper flange, a heat sink compound which has adhesive qualities at elevated temperatures was used. A PID controller and a solid state relay provides adequate control of the sample surface temperature to  $\pm 2^{\circ}\text{C}$  over an approximate temperature range of 30-120°C. The power source is a 120 volt variac, and a direct current rectifier converts the AC source to DC power such that a maximum voltage of 50 volts is supplied to the heating element. The elevated-temperature indentation experiments were conducted at temperatures ranging from 65-120°C. The elevated temperatures were expected to enhance differences in response between interphase and bulk matrix regions, because interphase regions often have lower glass transition temperatures,  $T_g$ , than the bulk matrix. After reaching the desired setpoint temperature, each sample was held at that temperature for at least one hour before indentation experiments were conducted. This procedure allowed the various parts of the AFM including the probe to reach thermal equilibrium, so that thermal expansion would not affect the indentation results.

## RESULTS AND DISCUSSION

### *Unsize carbon fiber-epoxy composite system*

Indentation response was measured on unsize carbon fiber-epoxy samples at 20, 65, 80, 100, and 120°C. In each case, several rows of indents were made from the bulk epoxy matrix toward and onto the fiber at various angles of approach. In general, the indentation response throughout each row was similar to the response measured on the bulk epoxy (i. e., at large distances from the fiber), as shown in Figures 3, 4, and 5. In each figure, all responses have been normalized by the average bulk epoxy response, as described in the Experimental section. The two horizontal lines represent the experimental scatter of the bulk epoxy responses, where the distance,  $4\sigma$ , between these lines represents  $\pm 2$  standard deviations about the average bulk epoxy response. Except for responses very close to the fiber, the responses measured within 6-7  $\mu\text{m}$  of the fiber fall within these  $\pm 2\sigma$  bands. No significant changes in response were observed with increasing temperature. Thus, any effects caused by a low  $T_g$  fiber-matrix interphase region were not observed for this composite system. This result might be due to the extremely small interphase region predicted for this combination of materials<sup>1, 5</sup>.

Within approximately 200 nm of the fiber surface, deformation was significantly restricted by the presence of the fiber because the fiber modulus is much greater than the matrix modulus. Using Equation 1, an apparent stiffening of the matrix material is observed. For example, the two data points in Figure 3 for which the calculated stiffnesses are significantly higher than the bulk response represent indents made approximately 40 and 70 nm, respectively, from the fiber. In the development of Equation 1, however, the indented material is assumed to have uniform properties which is obviously violated for indents that are influenced by the fiber. Thus, whether the stiffening effect is due just to the restriction of deformation near the fiber or a change in



the indentation mechanics caused by that restriction, the responses measured within 200 nm of the fiber cannot be considered as representative of an interphase effect.

#### *Sized copper-epoxy composite system*

Because the presence of the fiber tends to overwhelm effects due to interphase formation, a copper wire was coated with EPON 1001F and cured in a stoichiometric mixture of EPON 828 and PACM 20. Thus, the capability of the indentation technique to evaluate property changes across a coating-matrix interface or interphase could be studied. The coating procedure that was used produced a large coating on the copper wire that extended approximately 10  $\mu\text{m}$  from the fiber surface. Diffusion of amine into the coating occurs rapidly at a curing temperature of 80°C<sup>5</sup>, and amine will diffuse and equilibrate through the 10  $\mu\text{m}$  coating prior to gelation<sup>6</sup>. The stiffness difference between fully-cured EPON 1001F and EPON 828 is significant;  $E_{1001F}/E_{828} = 1.4$ <sup>5</sup>, as shown in Figure 1b. However, the epoxies are very similar and the stiffness difference is not so significant as to create a large stiffening effect, such as that observed near the fiber-epoxy interface. Because the coating was quite large, the responses of both the bulk epoxy and the "bulk" coating (measured approximately 5-7  $\mu\text{m}$  from the fiber) were characterized separately. These responses were then compared to the responses measured from indents made as a function of distance from the epoxy across the coating to the fiber.

Indentation responses were measured on the sized copper-epoxy system at 20, 65, 80, 100, and 120°C. As temperature increased, the plastic responses of the coating and matrix epoxies, as measured by the size of the indents, did not change significantly. This result is not surprising, because the  $T_g$  values of fully cured EPON 1001F and fully cured EPON 828 are approximately 150 and 160°C, respectively, as measured independently using dynamic mechanical analysis<sup>6</sup>. Also, for a given temperature, the indent sizes in the epoxy were very similar to those made in the coating.

Thus, Equation 1 was used to calculate the relative stiffnesses of the coating and matrix responses at each temperature assuming equivalent contact radii. From these calculations, the stiffness of the coating epoxy was approximately 1.3-1.4 times that of the matrix epoxy, which agrees with the estimated modulus ratio between fully cured EPON 1001F and fully cured EPON 828. This result is shown for 20, 65, 80, and 120°C in Figures 6-9. Again, all responses are normalized by the average response of the matrix epoxy, as described in the Experimental section. The two sets of two horizontal lines represent the experimental scatter of the bulk epoxy and bulk coating responses, i.e.,  $\pm 2$  standard deviations about the average responses of the bulk coating and bulk matrix epoxies, respectively.

The responses of the indents taken row by row from the epoxy through the coating to the fiber are also shown in Figures 6-9. Except near the fiber and through the coating-matrix interphase, the responses for distances of 0.5-7.5  $\mu\text{m}$  generally fall within the scatter from the bulk coating responses, i.e., responses of the coating material 5-7  $\mu\text{m}$  from the fiber that was measured separately from the data shown in these figures. Similarly, the responses for distances greater than 10  $\mu\text{m}$  from the fiber generally fall within the scatter from the bulk matrix responses. Near the fiber, a stiffening effect is observed in all cases.

The only responses that change significantly with temperature are that of the coating-matrix interphase region. At 20°C, the change in response moving from the bulk epoxy to the coating is not a step increase as idealized in Figure 1b, but rather a gradual increase in stiffness over a 1.0-1.5  $\mu\text{m}$  distance. Further, a band approximately 1.5  $\mu\text{m}$  wide was observed on topographic AFM images of this sample, such that the band formed a concentric cylinder about the copper wire at a distance of approximately 7.5-8.0  $\mu\text{m}$  from the wire. Thus, this region was somehow different from either the coating or the bulk epoxy, such that it was preferentially extracted during polishing. As temperature

increases from 20 to 65 °C (see Figures 6 and 7), at least a portion of the region becomes softer relative to the bulk epoxy, as instead of a gradual decrease in stiffness from the coating to the matrix, a nearly discontinuous change in stiffness is observed. This discontinuous change in stiffness is also apparent at 80°C, but a number of the measured responses in the coating-matrix interphase at 80°C have dropped below the  $-2\sigma$  line for the bulk epoxy. The response at 100°C (not shown) was similar to 80°C with a few more portions of the interphase having stiffnesses below that of the bulk epoxy.

The response of the interphase region at 120°C, however, is much different than the coating and matrix responses. For the entire region, the relative stiffness values are significantly lower than that of either the bulk matrix or coating epoxies. This result is a function of the differences in both elastic response and plastic response. For 20, 65, 80, and 100°C, all measured responses corresponded to indent sizes that did not change significantly within a given row. Thus, relative stiffnesses were calculated assuming equal contact radius values for each indent. At 120°C, the indent sizes in the interphase region were approximately 1.5 times larger than indent sizes in the epoxy or coating. This effect is shown in Figure 10. Assuming that the relative indent sizes are related to the relative contact radius values, a factor of 1.5 was used to relate the contact radius values of the interphase responses to that of the coating and matrix responses. Thus, the large differences in both elastic and plastic response of the interphase region compared to the bulk materials is represented in Figure 9. The increase in indent size with increasing temperature was also observed for a low  $T_g$  ( $T_g = 75^\circ\text{C}$ ) epoxy sample; for  $T < T_g$ , indent size did not change significantly with increasing temperature; as temperature increased above  $T_g$ , indent size increased by a factor of 1.2 for  $T = T_g + 5^\circ\text{C}$  and by a factor of 1.7 for  $T = T_g + 20^\circ\text{C}$ . Assuming that the temperature with respect to  $T_g$  has a similar effect on the indentation responses measured in the interphase region, the  $T_g$  values in the coating-matrix interphase of the copper wire sample range between 100°C and 120°C.

The measured changes in relative stiffness are expected to be related to variations in chemistry and/or microstructure that affect local modulus and  $T_g$  values.

A diffusion-reaction kinetics model was used to predict the compositional gradients that formed as the EPON 828 epoxy and PACM 20 amine diffused and cured within the EPON 1001F coating. A more complete description of this model can be found elsewhere<sup>20</sup>. The diffusion coefficient, or diffusivity, that characterizes the diffusion of epoxy into another epoxy was not available. However, from the results of the diffusion of epoxy and amine into a thermoplastic polymer, the diffusivity of the amine was calculated to be an order of magnitude higher than that of the epoxy<sup>21</sup>. Based on this result, a diffusivity was estimated for the diffusion of EPON 828 into EPON 1001F using the ratio of amine diffusivity to epoxy diffusivity for the thermoplastic polymer case along with the measured diffusivity of amine into EPON 1001F<sup>5</sup>. These diffusivities were then input into the model along with the epoxy-amine reaction kinetics measured by Skourlis<sup>5</sup>.

The resulting stoichiometry variations predicted throughout an 8  $\mu\text{m}$ -thick coating is shown in Figure 11. For this analysis, a maximum time of 12 min. was used because after 10-15 min., the diffusion process is altered by reaction such that further diffusion is limited as the gel point is approached<sup>5</sup>. After 12 min., the amine has diffused across the entire coating and, before the gel point is reached, a uniform concentration of amine will form such that the coating epoxy reacts with a stoichiometric amount of amine at each point throughout the coating. Because the diffusion of the EPON 828 epoxy is much slower than that of the amine, it will only diffuse a few microns into the coating prior to gelation, as shown in Figure 11. Some counter diffusion of the coating material out into the matrix epoxy might also occur. However, this effect is not included in the diffusion model. In any case, the original coating-matrix interface is replaced by an interphase region, the composition of which is difficult to define. From the diffusion

model results, the interphase region is predicted to contain both off-stoichiometry EPON 828 and off-stoichiometry EPON 1001F. Because of the assumptions of the model, the actual interphase composition might differ from the predicted composition. Most likely, the microstructure that develops in this region is significantly affected by the diffusion and reaction processes, such that a lower  $T_g$  interphase develops.

#### *Sized AS4-epoxy composite system*

The responses of the sized AS4-epoxy system were very similar to the responses of the unsized system. Four separate batches of samples were indented using several different probes. In each case, no change in indentation response was observed for distances of 200 nm up to 8  $\mu\text{m}$  from the fiber. The only observed change in indentation behavior was an increase in stiffness within 200 nm of the fiber, similar to that observed in the previous studies. This result was surprising considering the large difference observed between the coating and matrix responses in the sized copper wire system. In fact, for two different probes, consecutive sets of indents were made at room temperature, first on the sized AS4 system and then on the sized copper wire system. In both cases, the coating region of the copper wire system appeared to be significantly stiffer than the bulk matrix epoxy, whereas no change in indentation was measured on the sized AS4 system. Also, no topographic differences similar to the 1.5  $\mu\text{m}$  wide band observed in the sized copper wire system were observed after polishing the sized AS4 samples. Thus, the expected change in properties from the coating to the matrix is not observed, and changes in response due to interphase formation is also not observed.

Increasing temperature did not produce a measurable change in indentation response from either the coating-matrix interphase or the fiber-matrix interphase with one exception. The indentation response of a sized AS4-epoxy sample at 120°C is shown in Figure 12. The relative stiffness values for this data set were calculated using Equation 1 and assuming equal contact radius values for each indent. For the three data points

nearest the fiber, only two fall above the  $4\sigma$  epoxy band and are representative of the apparent stiffening of the material adjacent to the fiber. The third point represents a response that was similar elastically to the average bulk epoxy response (normalized stiffness = 1.0). However, the indent corresponding to this data point was significantly larger than the other indents. If the relative indent sizes are related to the relative contact radii, such as was assumed for the sized copper-epoxy system at 120°C, then the normalized stiffness corresponding to this data point would be approximately 0.85. Thus, the  $T_g$  of the fiber-matrix interphase of this system might again be between 100°C and 120°C. However, because only one indent exhibited this behavior, the conclusion of a lower  $T_g$  interphase region for this system might not be valid.

As commented on previously, the lack of two distinguishable responses from the coating and the matrix epoxies is surprising considering that interphase formation models have predicted a significant change in properties from the coating to the matrix (see Figure 1b) similar to that measured in the copper-epoxy system. However, these models assume that only amine diffuses into the coating. Results of the diffusion-reaction kinetics model indicated that, for the copper-epoxy system, the coating-matrix interphase might have formed because of diffusion of matrix epoxy into the coating epoxy. Using this model for a 1  $\mu\text{m}$  coating, the amine easily diffuses to the fiber and reaches a nearly constant concentration through the coating after just 12 min., as shown in Figure 13. Although the epoxy diffuses much more slowly, it is also able to reach the fiber and might also reach a nearly constant concentration through the coating prior to gelation. A relatively uniform microstructure could then develop around the fiber such that the network structure includes both EPON 828 and EPON 1001F prepolymers linked by amine crosslinks. This result would explain the fairly constant indentation responses for the sized AS4-epoxy system.

## CONCLUSIONS

The AFM indentation techniques was used to investigate the local indentation responses of several polymer composite systems. In each case, the calculated relative stiffnesses were significantly higher for indents that were less than 200-300 nm from the fiber. This stiffening effect is caused by the restriction imposed by the fiber to the adjacent matrix material and might be related to a change in indentation mechanics due to the presence of the fiber. Although the fiber-matrix interphase for these systems is expected to have a lower  $T_g$  than the matrix epoxy, the stiffening effect was still present at temperatures greater than the predicted interphase  $T_g$ .

The inability to produce indents near the fiber that are unaffected by the presence of the fiber clearly limits the application of this technique for probing fiber-matrix interphase regions in composite systems. However, this technique has been useful for investigating systems in which a polymer-polymer interface or interphase is expected to form. For the two composite systems that incorporated sized fibers, unexpected property variations were discovered. For the 8  $\mu\text{m}$  sizing on the copper wire, an interphase region formed between the coating and matrix epoxies which had a lower  $T_g$  than the bulk regions. The relative stiffness of the bulk coating to the bulk matrix was similar to the modulus ratio between the two stoichiometrically cured epoxies. For the 1  $\mu\text{m}$  sizing on the carbon fiber, no change in indentation response with distance from the fiber was observed for temperatures ranging from 20°C up to 120°C. Both sets of results were explained using a diffusion-reaction kinetics model in which the matrix epoxy was allowed to diffuse into the coating epoxy. While the amine completely diffuses across the two coatings, the epoxy diffusion is much slower. Thus, for the 8  $\mu\text{m}$  sizing, an interphase region forms, while for the 1  $\mu\text{m}$  sizing, the two epoxies completely mix.

## ACKNOWLEDGMENTS

The authors are grateful for the financial support of the U. S. Army Research Laboratory (ARL) under the Composite Materials Research Collaborative Program (CMR), ARL agreement number DAAL01-96-2-0048. Also, a special thanks goes out to Rod Don of the Center for Composite Materials for his help in the design and debugging of the heating stage.

## References

1. Beck Tan, N., McKnight, S. H., and Palmese, G. R., "Chemical Segregation in Epoxy Precursor Mixtures at Simulated Fiber/Matrix Interfaces," in *Proceedings of the American Chemical Society -- Division of Polymeric Materials: Science and Engineering* **77** (1997) 640-641.
2. Boerio, F. J. and Hong, P. P., "Non-destructive Characterization of Epoxy-Dicyandiamide Interphases Using Surface-enhanced Raman Scattering," *Mater. Sci. Eng.* **A126** (1990) 245-252.
3. Sellitti, C., Koenig, J. L., and Ishida, H., "Surface Characterization of Carbon Fibers and Interphase Phenomena in Epoxy-reinforced Composites," *Mater. Sci. Eng.* **A126** (1990) 235-244.
4. Palmese, G. R. and McCullough, R. L., "Kinetic and Thermodynamic Considerations Regarding Interphase Formation in Thermosetting Composite Systems," *J. Adhesion*, **44** (1994) 29-49.
5. Skourlis, T. P., "Structure and Properties of the Interphase in Coated Carbon-Fiber/Epoxy Systems," PhD thesis (University of Delaware, USA, 1996).
6. VanLandingham, M. R., "Characterization of Interphase Regions in Fiber-Reinforced Polymer Composite Materials," PhD Thesis (University of Delaware, USA, 1997).



7. Skourlis, T. P. and McCullough, R. L., "The Effect of Temperature and Fiber Coatings on the Behavior of the Interphase in Composite Materials," in *Proceedings of the American Society for Composites Eighth Technical Conference* (1993) 218-226.
8. Skourlis, T. P. and McCullough, R. L., "The Effect of Temperature on the Behavior of the Interphase in Polymeric Composites," *Composites Sci. Technol.* **49** (1993) 363-368.
9. Williams, J. G., Donnellan, M. E., James, M. R., and Morris, W. L., "Properties of the Interphase in Organic Matrix Composites," *Mater. Sci. Eng.* **A126** (1990) 305-312.
10. Williams, J. G., James, M. R. and Morris, W. L., "Formation of the Interphases in Organic-Matrix Composites," *Composites* **25** (1994) 757-762.
11. Sottos, N. R., Scott, W. R., and McCullough, R. L., "Micro-interferometry for Measurement of Thermal Displacements at Fiber/Matrix Interfaces," *Exper. Mechanics* **32** (1991) 98-103.
12. Asloun, E. M., Nardin, M., and Schultz, J., "Stress Transfer in Single-Fibre Composites: Effect of Adhesion, Elastic Modulus of Fibre and Matrix, and Polymer Chain Mobility," *J. Mater. Sci.* **24** (1989) 1835-1844.
13. Hrivnak, J., Dagastine, R. R., and McCullough, R. L., "Interphase Effect on Intralaminar Fracture Toughness," in *Proceedings of the Nineteenth Annual Adhesion Society Conference* (1996).
14. Garton, A., Stevenson, W. T. K., and Wang, S., "Interfacial Reactions in Carbon-Epoxy Composites," *British Polym. J.* **19** (1987) 459-465.
15. Drzal, L. T., Rich, M. J., and Koenig, M. F., and Lloyd, P. F., "Adhesion of Graphite Fibers to Epoxy Matrices: II The Effect of Fiber Finish," *J. Adhesion* **16** (1983) 133-152.

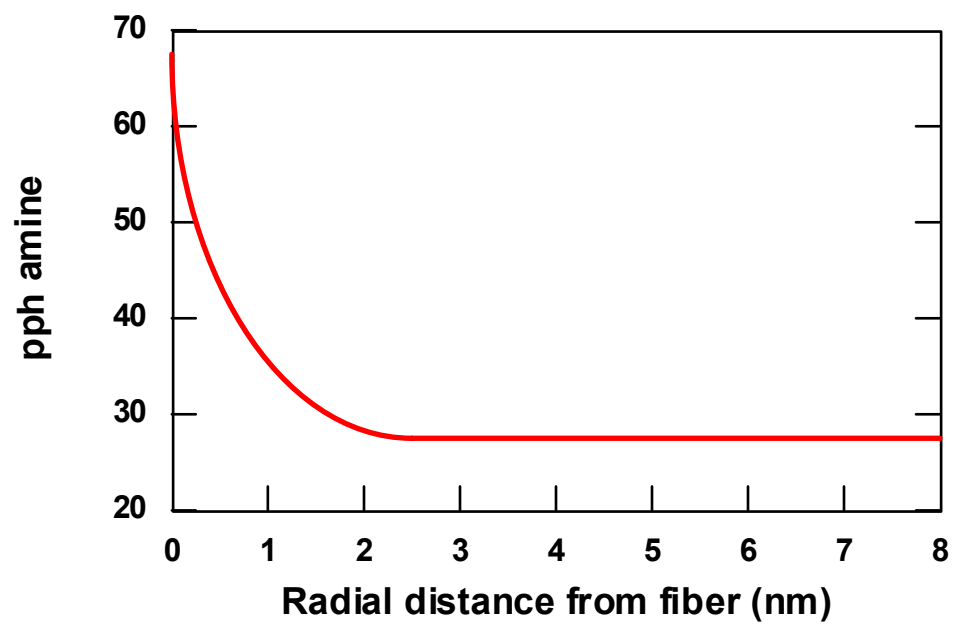
16. VanLandingham, M. R., McKnight, S. H., Palmese, G. R., Eduljee, R. F., Gillespie, J. W., Jr., and McCullough, R. L., "Relating Elastic Modulus to Indentation Response Using Atomic Force Microscopy," *J. Mater. Sci. Lett.* **16** (1997) 117-119.
17. VanLandingham, M. R., McKnight, S. H., Palmese, G. R., Elings, J. R., Huang, X., Bogetti, T. A., Eduljee, R. F., and Gillespie, J. W., Jr., "Nanoscale Indentation of Polymer Systems Using the Atomic Force Microscope," *J. Adhesion* **64** (1997) 31-59.
18. Bolshakov, A., Oliver, W. C., and Pharr, G. M., "An Explanation for the Shape of Nanoindentation Unloading Curves Based on Finite Element Simulation," in *Thin Films: Stresses and Mechanical Properties V*, Materials Research Society Proceedings **356** (1995) 675-680.
19. Dagastine, R. R., "Interrogating the Interphase Region in Fiber Reinforced Composites Using Atomic Force Microscopy," BS thesis (University of Delaware, USA, 1997).
20. Rajagopalan, G., "Diffusion of Reacting Thermosets into Thermoplastics," PhD Thesis (University of Delaware, USA, 1998)..
21. Immordino, K. M., McKnight, S. H., and Gillespie, J. W., Jr., "In situ Evaluation of the Diffusion of Epoxy and Amine in Thermoplastic Polymers," in *Proceedings of the 54th Technical Conference of the Society of Plastics Engineers* **402** (1996) 1214-1218.

### Figure Captions

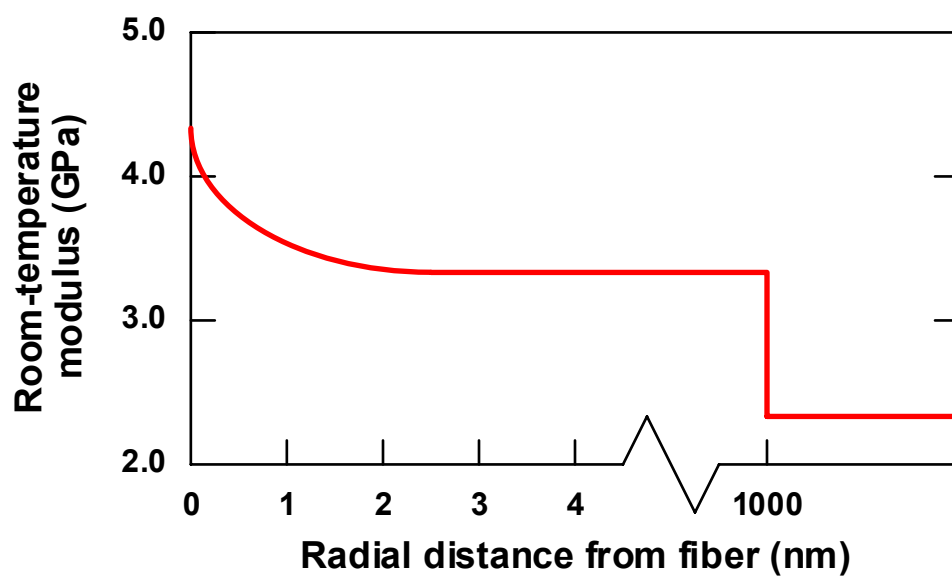
Figure 1      (a) Stoichiometric gradient near the fiber surface due to preferential amine absorption, and (b) room-temperature modulus as a function of distance from the fiber surface for a 1  $\mu\text{m}$ -sized fiber (fiber sizing is EPON 1001F)<sup>5</sup>.

- Figure 2 Schematic of the AFM heating stage (insulation not shown). The probe is mounted to the bottom of the piezo actuator.
- Figure 3 Indentation response at 20°C as a function of distance from the fiber for the unsized AS4-epoxy system. Relative stiffness values are normalized with respect to that of the bulk epoxy matrix material.
- Figure 4 Indentation response at 80°C as a function of distance from the fiber for the unsized AS4-epoxy system. Relative stiffness values are normalized with respect to that of the bulk epoxy matrix material at 80°C.
- Figure 5 Indentation response at 120°C as a function of distance from the fiber for the unsized AS4-epoxy system. Relative stiffness values are normalized with respect to that of the bulk epoxy matrix material at 120°C.
- Figure 6 Indentation response at 20°C as a function of distance from the fiber for the sized copper-epoxy system. Relative stiffness values are normalized with respect to that of the bulk epoxy matrix material.
- Figure 7 Indentation response at 65°C as a function of distance from the fiber for the sized copper-epoxy system. Relative stiffness values are normalized with respect to that of the bulk epoxy matrix material at 65°C.
- Figure 8 Indentation response at 80°C as a function of distance from the fiber for the sized copper-epoxy system. Relative stiffness values are normalized with respect to that of the bulk epoxy matrix material at 80°C.
- Figure 9 Indentation response at 120°C as a function of distance from the fiber for the sized copper-epoxy system. Relative stiffness values are normalized with respect to that of the bulk epoxy matrix material at 120°C.
- Figure 10 AFM image of 120°C indents across coating-matrix interphase in the sized copper wire sample. Height scale from black to white is 0 to 50 nm.

- Figure 11      Diffusion-reaction kinetics model of the diffusion of EPON 828 epoxy and PACM 20 amine into an 8  $\mu\text{m}$ -thick coating. The concentrations of amine and epoxy are normalized with respect to their bulk concentrations. At 12 min., the diffusion process begins to be altered by reaction such that further diffusion is limited as the gel point is approached.
- Figure 12      Indentation response at 120°C as a function of distance from the fiber for the sized AS4-epoxy system. Relative stiffness values are normalized with respect to that of the bulk epoxy matrix material at 120°C.
- Figure 13      Diffusion-reaction kinetics model of the diffusion of EPON 828 epoxy and PACM 20 amine into a 1  $\mu\text{m}$ -thick coating. The concentrations of amine and epoxy are normalized with respect to their bulk concentrations. At 12 min., the diffusion process begins to be altered by reaction such that further diffusion is limited as the gel point is approached.



(a)



(b)

Figure 1 VanLandingham, et al.

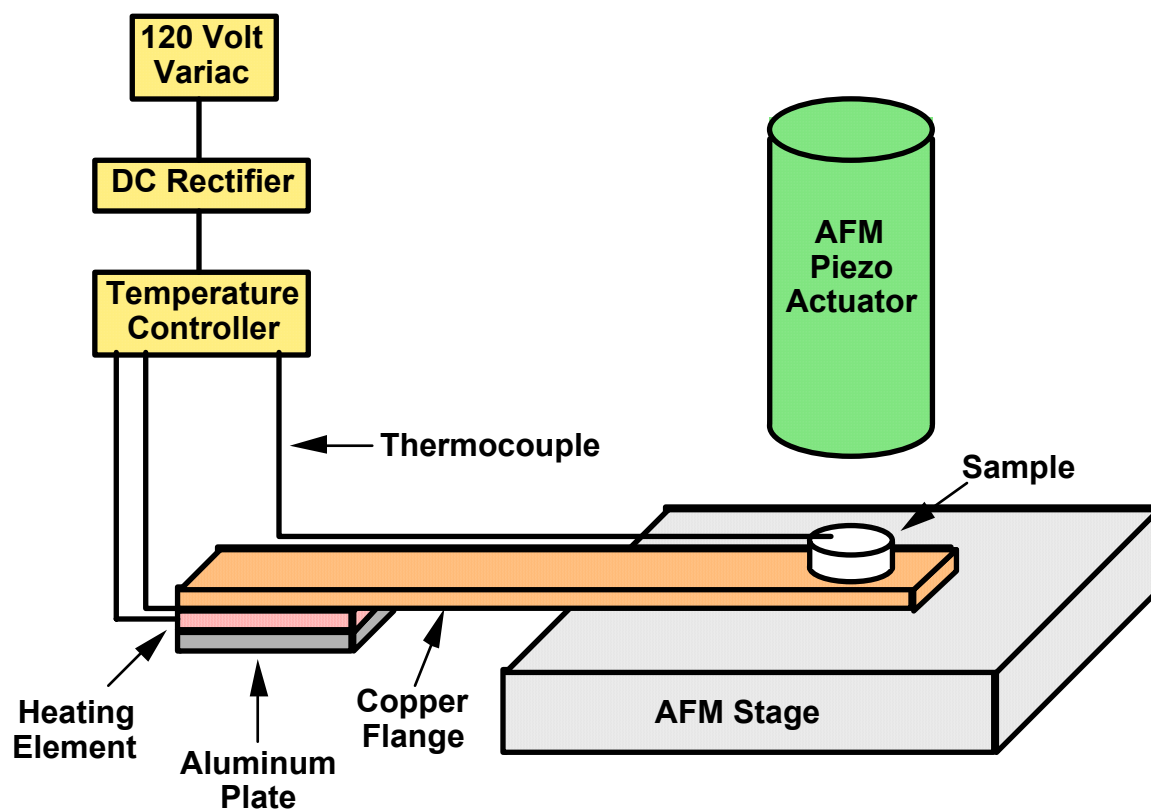


Figure 2 VanLandingham, et al.

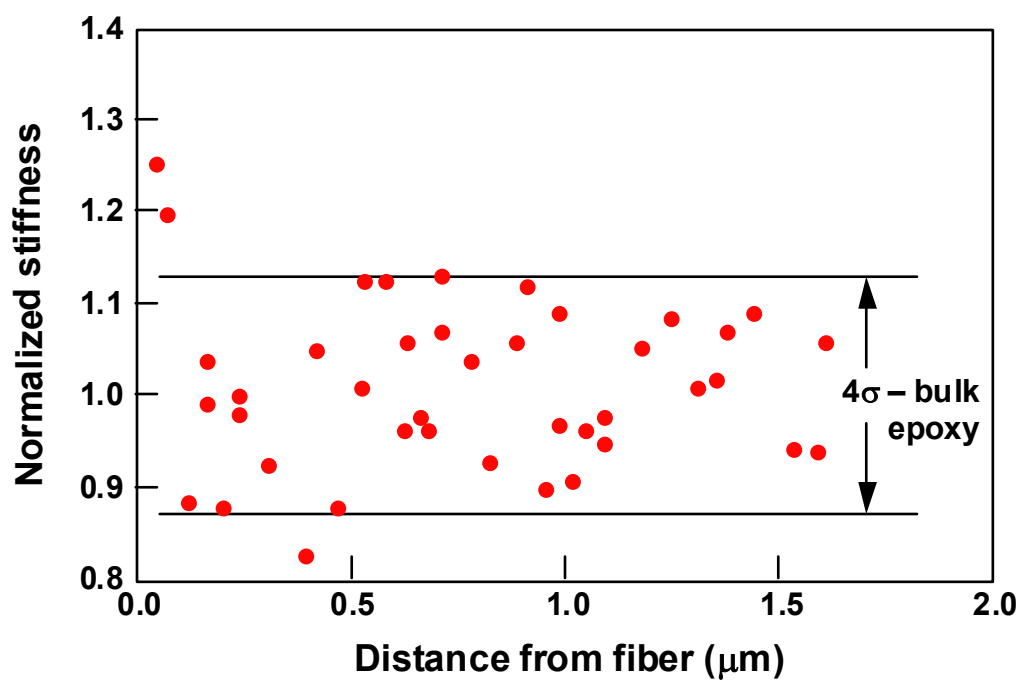


Figure 3 VanLandingham, et al.

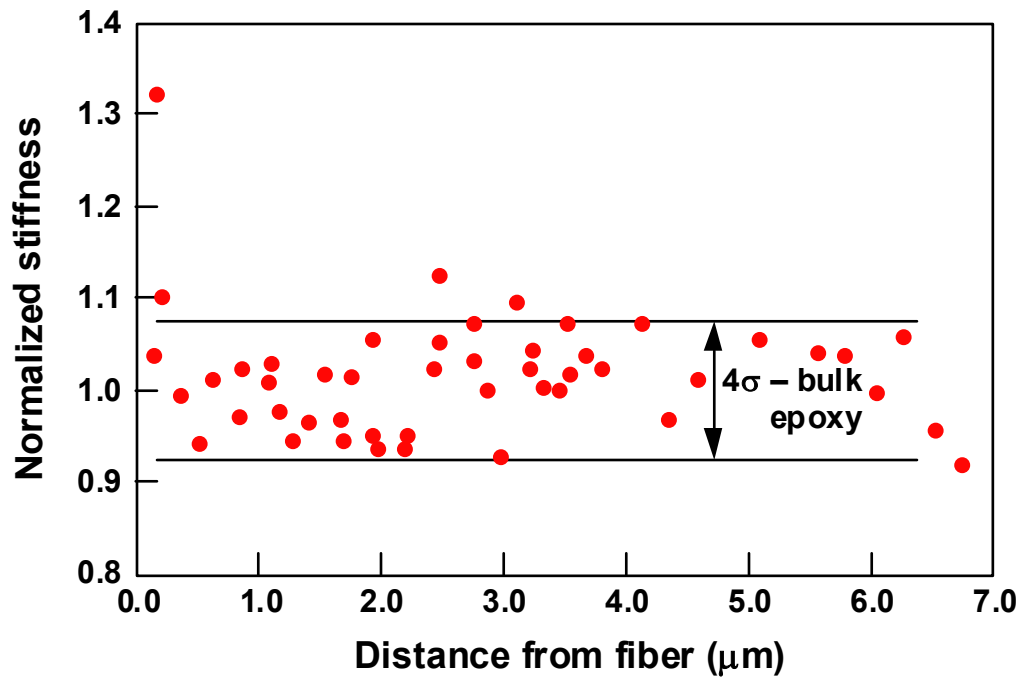


Figure 4 VanLandingham, et al.



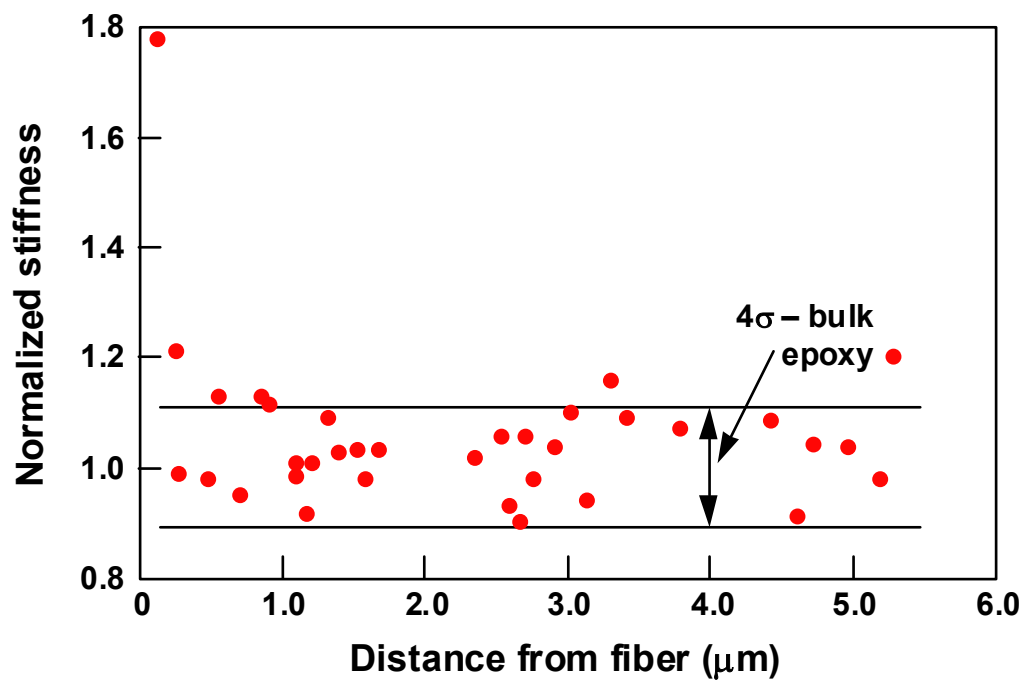


Figure 5 VanLandingham, et al.

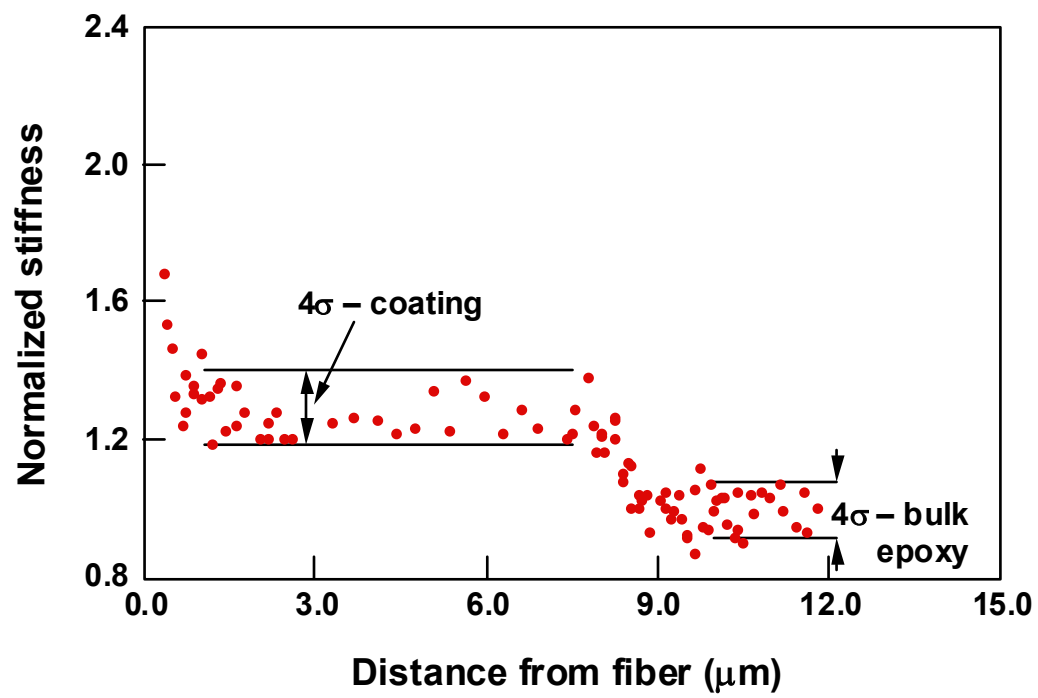


Figure 6 VanLandingham, et al.

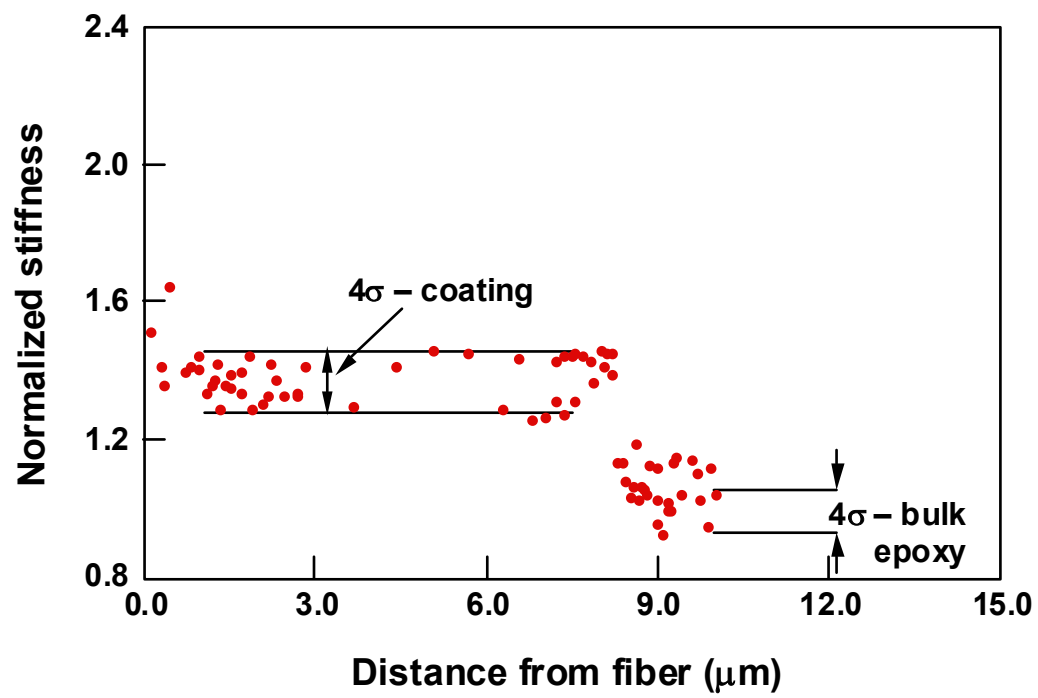


Figure 7 VanLandingham, et al.

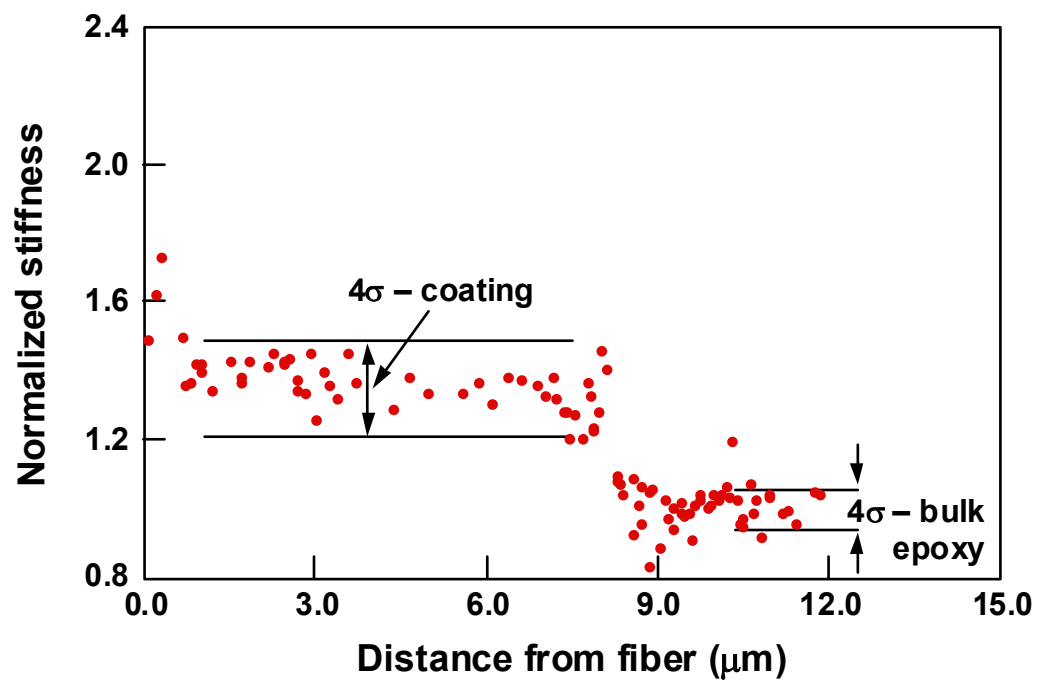


Figure 8 VanLandingham, et al.

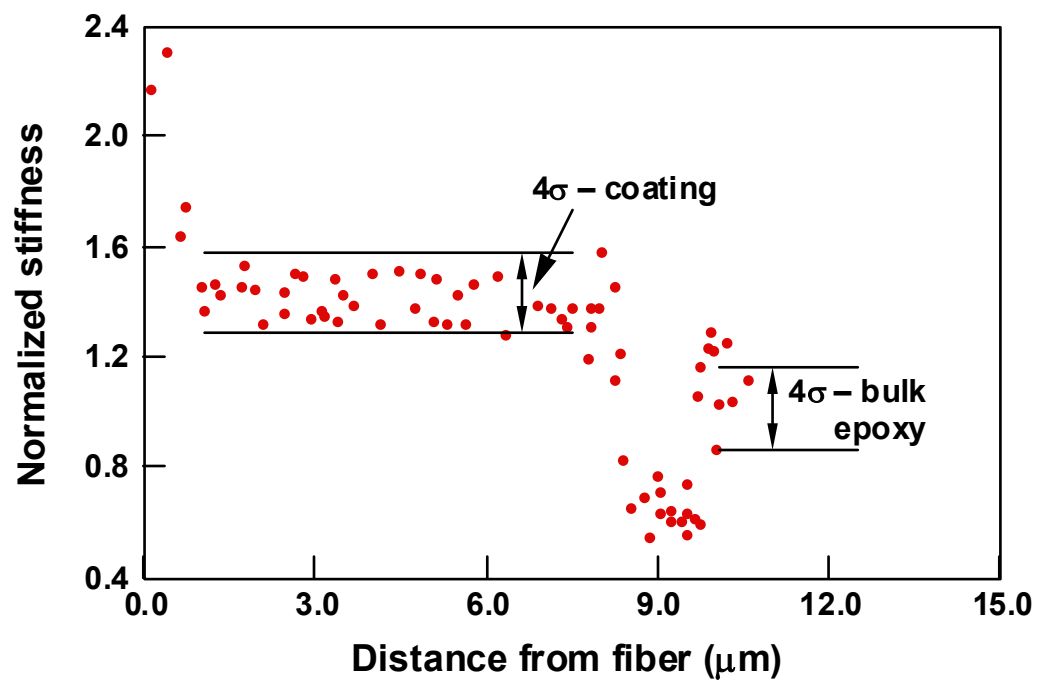


Figure 9 VanLandingham, et al.

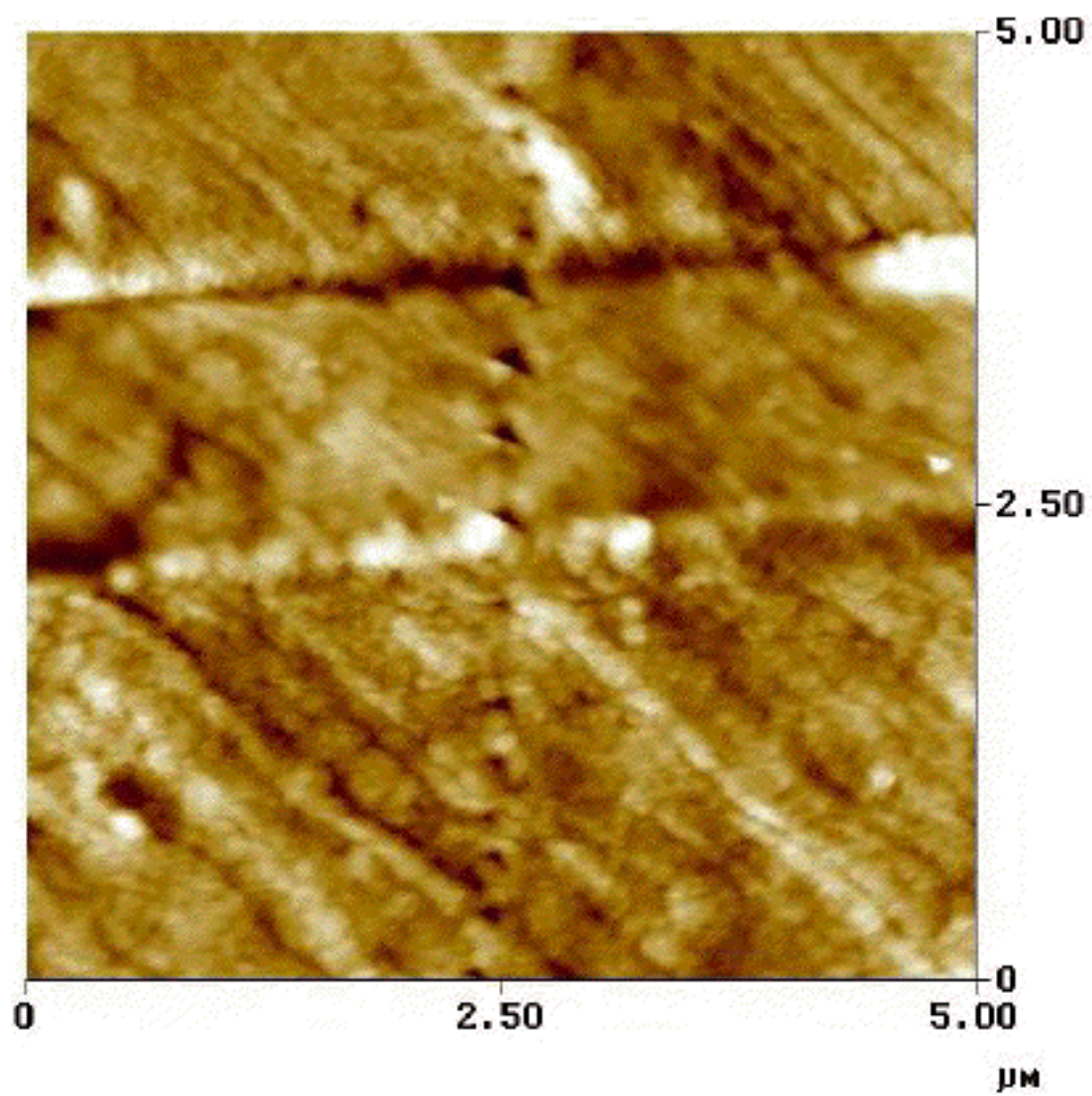


Figure 10 VanLandingham, et al.

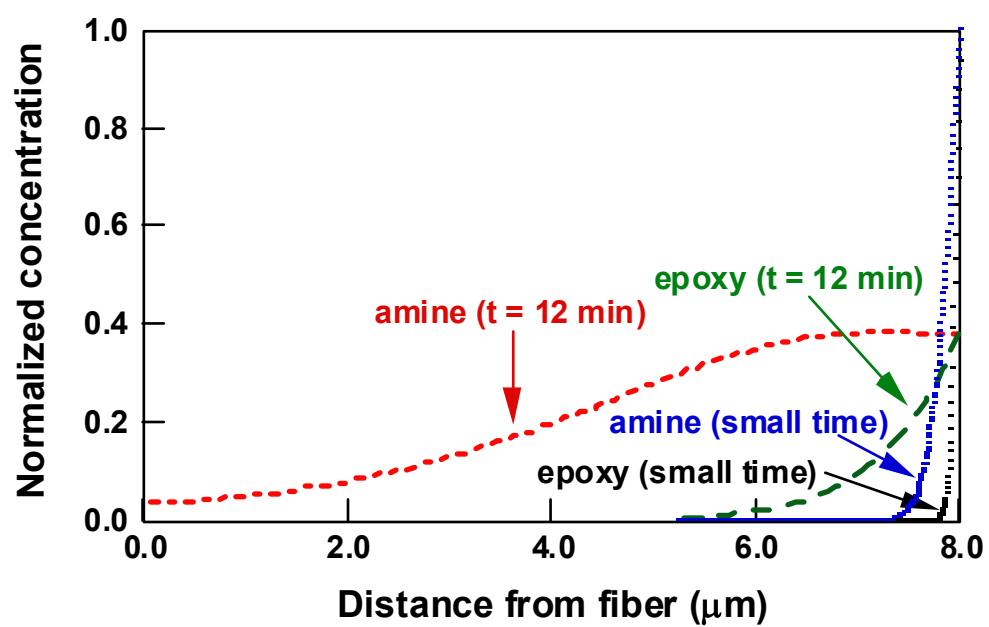


Figure 11 VanLandingham, et al.

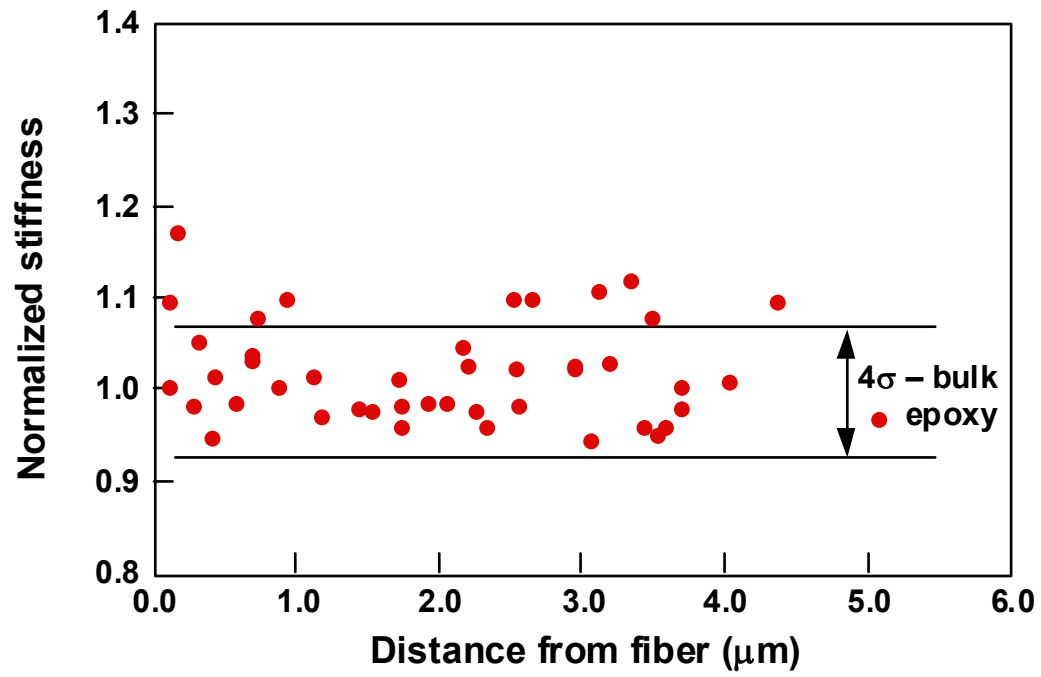


Figure 12 VanLandingham, et al.



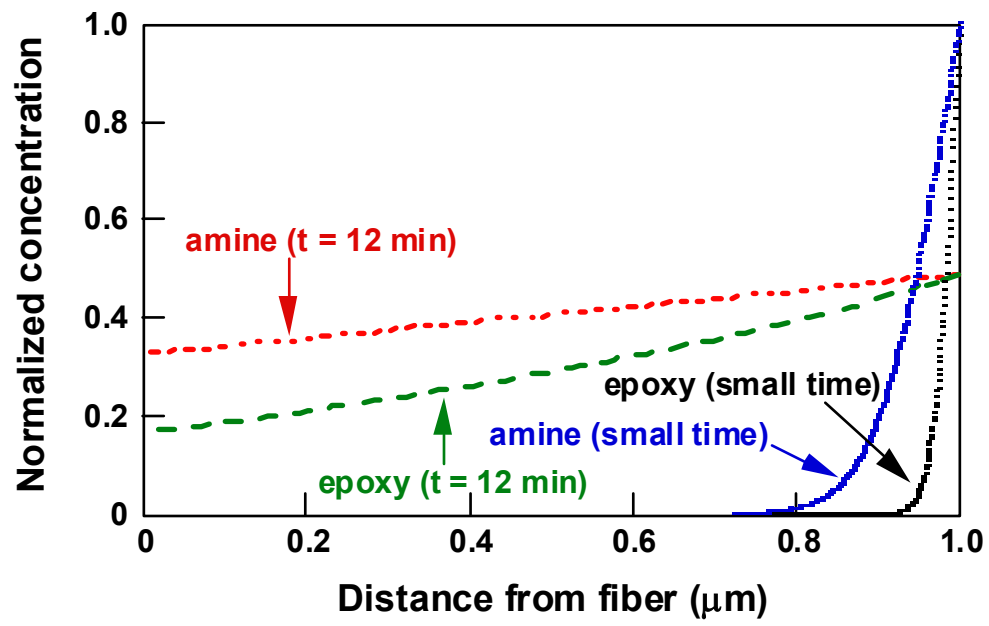


Figure 13 VanLandingham, et al.